

Conduction-Band Surface Plasmons in the Electron-Energy-Loss Spectrum of GaAs(110)

R. Matz and H. Lüth

II. Physikalisches Institut der Rheinisch-Westfälischen, Technischen Hochschule Aachen, D-5100 Aachen, Federal Republic of Germany

(Received 15 December 1980)

Apart from Fuchs-Kliewer surface phonons, conduction-band surface plasmons and probably intraband single-particle scattering contribute to the electron-energy-loss spectra (primary energy ~ 5 eV, resolution < 10 meV) measured on clean, UHV-cleaved, n -type GaAs(110) surfaces. Coupling between surface phonons and plasmons derives from frequency shifts which depend on surface carrier concentration.

PACS numbers: 71.45.Gm, 79.20.Kz

High-resolution electron-energy-loss spectroscopy (HRELS) has recently been applied very successfully to the study of vibrations of adsorbates on metal surfaces. There has, however, been little research in the field of semiconductor surfaces. On compound semiconductors the multiple excitation of Fuchs-Kliewer surface phonons¹ makes it hardly possible to observe adsorbate-substrate vibrations close to the elastic peak.^{2,3} In this paper we demonstrate that on semiconductor surfaces, electronic excitations in the energy range below 100 meV also have to be taken into account in HRELS: Collective excitations of the conduction-band electrons, surface plasmons, can be observed. Because of the small electronic effective mass, GaAs is ideally suitable for studying the coupling between surface plasmons and phonons in the usual carrier-concentration range. The effects may be of interest to the study of free carriers and transport properties near the surface. In adsorption studies additional information about the space-charge layer can be obtained.

The samples were prepared from single-crystal bars of n -type GaAs (Te-doped: $n = 4.3 \times 10^{17}$ and $9 \times 10^{17} \text{ cm}^{-3}$, $\mu \approx 3000 \text{ cm}^2/\text{V s}$; Si-doped: $n = 3.1 \times 10^{17} \text{ cm}^{-3}$, $\mu \approx 3000 \text{ cm}^2/\text{V s}$). The bulk carrier concentrations n were determined by Hall-effect measurements. Furthermore, samples with negligible carrier concentration at 300 K were prepared from semi-insulating, Cr-doped material (p type) with specific resistivities above $10^6 \Omega \text{ cm}$. The double-wedge technique was used for cleavage in ultrahigh vacuum ($p < 10^{-8} \text{ Pa}$).

Electron-energy-loss spectra were recorded in the direction of the specular beam with a primary electron energy of 5 eV. The single-stage spectrometer used (resolution: 7 meV at $3 \times 10^{-11} \text{ A}$ current at multiplier, without sample) is of the 127° deflector type described previously.²

On clean cleaved (110) surfaces of semi-insulat-

ing GaAs, a series of energetically equidistant loss and gain peaks is found [Fig. 1(a)]. The energetic distance between the multiple-excitation bands amounts to $36.2 \pm 0.2 \text{ meV}$, the excitation energy of Fuchs-Kliewer surface phonons.³

Loss spectra measured on n -type material exhibit a different spectral shape. On clean cleaved surfaces, and also after exposure to small dosages of dissociated hydrogen (up to 1 L) [1 langmuir (L) = 10^{-6} Torr sec] or to residual gas, spectra as in Fig. 1(b) (curve in full line) are measured. A series of loss and gain peaks is observed at energies $\hbar\omega_{\pm}$ resembling those of the phonon peaks in Fig. 1(a) (slightly shifted up in energy). Additional gains and losses (including multiples) emerge with a considerably smaller quantum energy $\hbar\omega_{\pm}$. The positions of some clearly resolved loss peaks are plotted in Fig. 2 in the following way: Open symbols are used for clean surfaces with negligible residual gas exposure; full symbols for a 1-L exposure to residual gas or dissociated H_2 . Different bulk doping is distinguished by different symbols. The abscissa is an effective electron density n' which determines the position of the two losses at $\hbar\omega_{-}$ and $\hbar\omega_{+}$. A 1-L gas exposure obviously shifts the peaks down in energy towards peak positions measured on samples with weaker doping. This is confirmed by measurements after higher dosages (10 to 100 L) of dissociated H_2 : Only the phononlike excitation survives shifting to the energy already known from the semi-insulating samples. But still the spectrum looks more similar to the one shown in Fig. 1(b) than in Fig. 1(a), indicating a remaining strong damping of the phonon. Bulk electron densities n (measured by Hall effect) have been used to plot the experimental points of the clean Te-doped samples in Fig. 2. After inserting the points for the contaminated surfaces by interpolation one has to assume an effective surface electron concentra-

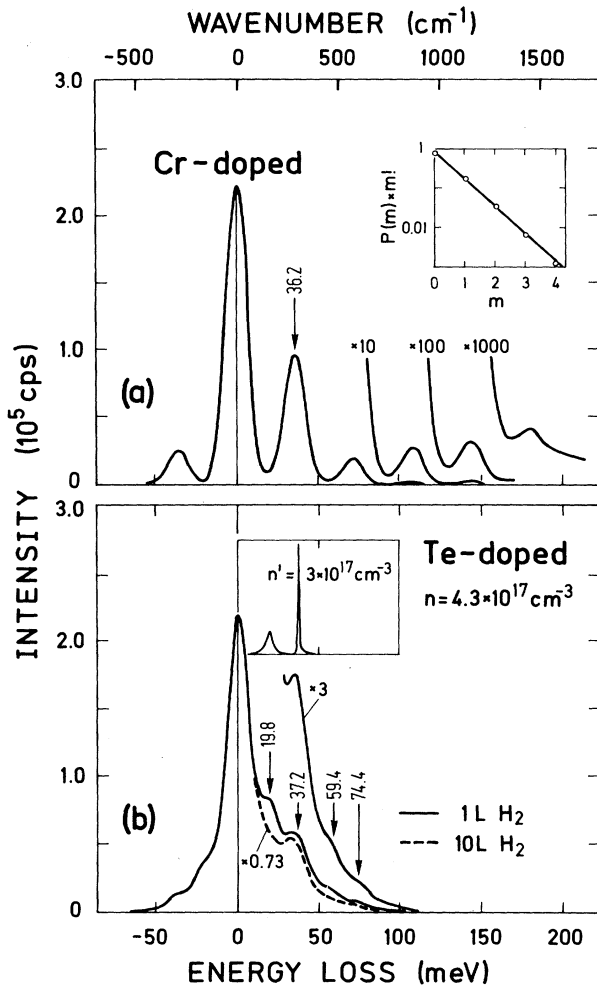


FIG. 1. (a) Loss spectrum of a clean cleaved semi-insulating surface (angle of incidence $\theta = 80^\circ$). Inset: The loss intensities I_m obey a Poisson distribution law $P(m) = I_m / \sum I_m = (m!)^{-1} Q^m \exp(-Q)$. (b) Loss spectra measured on an n -type sample after exposures to atomic hydrogen (angle of incidence $\theta = 70^\circ$; H dosages unknown; H₂ dosages: 1 and 10 L). Inset: Calculated surface loss function $-\text{Im}(1 + \epsilon)^{-1}$ in arbitrary units; $\epsilon(\omega)$ according to Eq. (1) with an effective electron density $n' = 3 \times 10^{17} \text{ cm}^{-3}$.

tion n' for the clean Si-doped sample of $2 \times 10^{17} \text{ cm}^{-3}$ rather than $3 \times 10^{17} \text{ cm}^{-3}$ (the bulk density n) to achieve a reasonable fit to this scheme; this is in contrast to the assumption $n' = n$ on clean Te-doped samples.

Within the framework of dielectric theory for surface scattering⁴ the shape of the loss spectrum is essentially determined by the surface loss function $-\text{Im}[\epsilon(\omega) + 1]^{-1}$ as far as multiple excitations are excluded. For semi-insulating

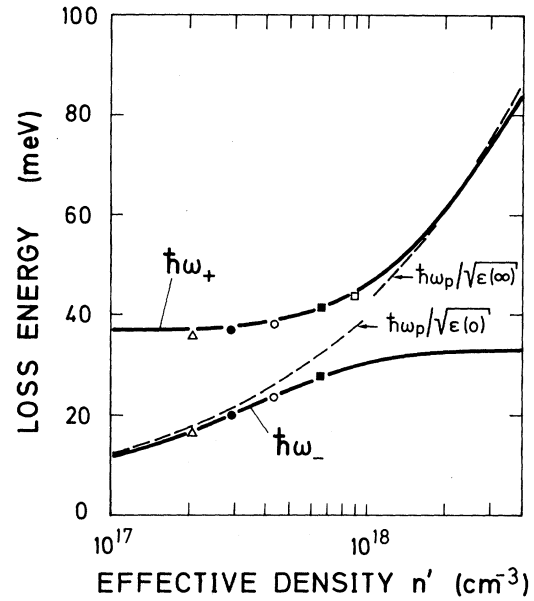


FIG. 2. Loss-peak positions $\hbar\omega_+$ and $\hbar\omega_-$ calculated from the surface loss function with $\epsilon(\omega)$ according to Eq. (1) (curves in full line). Broken line: plasmon frequency without phonon coupling. The experimental points are obtained on samples with different doping: (a) Te-doped (bulk density, $n = 9 \times 10^{17} \text{ cm}^{-3}$): open square, clean; full square, after exposure to 1-L residual gas. (b) Te-doped (bulk density, $n = 4.3 \times 10^{17} \text{ cm}^{-3}$): open circle, clean; full circle, after exposure to 1-L dissociated H₂. (c) Si-doped (bulk density, $n = 3 \times 10^{17} \text{ cm}^{-3}$): open triangle, clean.

material $\epsilon(\omega)$ is the complex bulk dielectric function in the spectral range of the reststrahlen band.⁵ With this $\epsilon(\omega)$ the surface loss function yields a surface-phonon peak at 36.6 meV, which agrees reasonably well with the experimental value of 36.2 meV [Fig. 1(a)].

In contrast, on n -type material, $\epsilon(\omega)$ in the spectral range of the infrared- (IR-) active phonons is also influenced by free electrons in the conduction band. In the simplest approximation this contribution is described by the Drude model. Taking into account both the lattice oscillator (first term) and the free-electron contribution (second term) the total complex dielectric function is

$$\epsilon(\omega) = \epsilon(\infty) + [\epsilon(0) - \epsilon(\infty)] \frac{\omega_{TO}^2}{\omega_{TO}^2 - \omega^2 - i\omega\gamma} - \left(\frac{\omega_P}{\omega}\right)^2 \frac{1}{1 - 1/i\omega\tau} \quad (1)$$

$\epsilon(0)$ and $\epsilon(\infty)$, the static and the electronic dielectric constants, as well as the frequency of the

transverse-optical phonon ω_{TO} and the damping constant γ are taken from IR data.⁵ Mobility data μ of the deliverer and the electronic effective mass $m_n^* = 0.068m_0$ ⁶ were used to calculate the Drude relaxation time $\tau = m_n^* \mu / e$. Then $\epsilon(\omega)$ in Eq. (1) only depends on the electron density n in the conduction band via the bulk plasmon frequency

$$\omega_p^2 = ne^2 / \epsilon_0 m_n^*. \quad (2)$$

For a density of $3 \times 10^{17} \text{ cm}^{-3}$ the surface loss function calculated from Eq. (1) reflects the energetic positions of the single excitations in the experimental spectrum [Fig. 1(b), inset]. In Fig. 2 the two calculated peak positions $\hbar\omega_-$ and $\hbar\omega_+$ (solid lines) are plotted versus carrier concentration n' for comparison with the experimental peak positions discussed before. For small n' , $\hbar\omega_-$ is surface-plasmon-like and $\hbar\omega_+$ surface-phonon-like. Near $n' = 10^{18} \text{ cm}^{-3}$ the two branches interchange their character thus indicating a coupling between the two modes via their electric field.

For the present experiments carrier concentrations within the penetration depth of the surface phonon and the plasmon, respectively ($\approx 300 \text{ \AA}^3$), i.e., essentially within the space charge layer, are relevant. The effective n' can therefore be varied both by bulk doping and by a change of the band bending due to gas adsorption. On clean cleaved Te-doped samples with low step densities, flat bands occur⁷ and the bulk carrier concentration coincides with that of the space-charge layer near the surface (Fig. 2, open square and open circle). Hydrogen adsorption bends the bands upwards and electrons are depleted near the surface, i.e., the effective carrier concentration n' is reduced below the bulk value n (full square and full circle). On clean cleaved Si-doped samples the disagreement between bulk and surface carrier concentrations obtained from Hall effect and from surface plas-

mon frequency, respectively, is explained by band bending due to surface defects⁷ (open triangle). Vice versa, the satisfying agreement between experimental and theoretical loss energies in Fig. 2 gives evidence for a flat-band situation on clean cleaved Te-doped samples, and for a depletion layer after hydrogen adsorption and on clean cleaved Si-doped samples.

Phonon and plasmon are accompanied by electric fields of the same wavelength. With decreasing wavelength λ the screening of this field in the free-electron gas becomes less effective and finally for $\lambda \ll \lambda_s$, the screening length, the collective response of the electron gas has disappeared; the excitations at $\hbar\omega_-$ and $\hbar\omega_+$ decay into single-particle excitations, i.e., intraband electron-hole pair excitation is favored. The screening wave vector $q_s = 2\pi/\lambda_s$ for the conduction-band electrons treated as a Boltzmann gas has the Debye form

$$q_s^2 = m_n^* \omega_p^2 / \epsilon(\infty) k_B T \quad (3)$$

and is of the order of 10^6 cm^{-1} . Since the maximum q transfer (resulting from energy and wave-vector conservation⁸) is of the same order of magnitude for a 20-meV plasmon in the present experiments, beside plasmon and phonon also intraband electron-hole-pair excitation is expected to contribute to the spectra. Assuming that this intraband scattering can also be described in terms of the dielectric theory, one can try to calculate both plasmon and intraband scattering by using the wave-vector-dependent Lindhard dielectric function $\epsilon(\omega, q)$ instead of the Drude term in Eq. (1) which is valid for $q = 0$.⁹ In this model the wave-vector dependence is caused by the conduction-band electrons only. Since now the surface loss function depends via q transfer on the scattering direction, an integration over the acceptance solid angle of the energy analyzer has to be performed. The appropriate expression for the scattering efficiency is given by Mills in a quantum-mechanical theory¹⁰ as

$$\frac{1}{|R|^2} \frac{d^2 S}{d\Omega d(\hbar\omega)} = \frac{m^2 e^2 v_{\perp}^2}{\hbar^4 \pi^3 \cos \theta} \frac{k_s}{k_I} [N(\omega) + 1] \frac{v_{\perp}^2 q_{\parallel}}{[v_{\perp}^2 q_{\parallel}^2 + (\omega - \vec{v}_{\parallel} \cdot \vec{q}_{\parallel})^2]^2} \text{Im} \frac{-1}{1 + \epsilon(\omega, q_{\parallel})}. \quad (4)$$

Integration of Eq. (4) yields the loss intensity $dS/d(\hbar\omega)$ (in meV^{-1}) normalized to the elastically reflected intensity. The convolution of $dS/d(\hbar\omega)$ with an assumed Gaussian-shaped transmission function (full width at half maximum: 12 meV) of the analyzer, therefore, should be comparable to a measured loss spectrum. In this way the

spectrum on semi-insulating material can be calculated in good agreement with the experimental curve [Fig. 1(a), without multiple losses] when the free-electron contribution in $\epsilon(\omega, q)$ is neglected. In Fig. 3 two calculated spectra for carrier concentrations of $4.3 \times 10^{17} \text{ cm}^{-3}$ and 0.8°

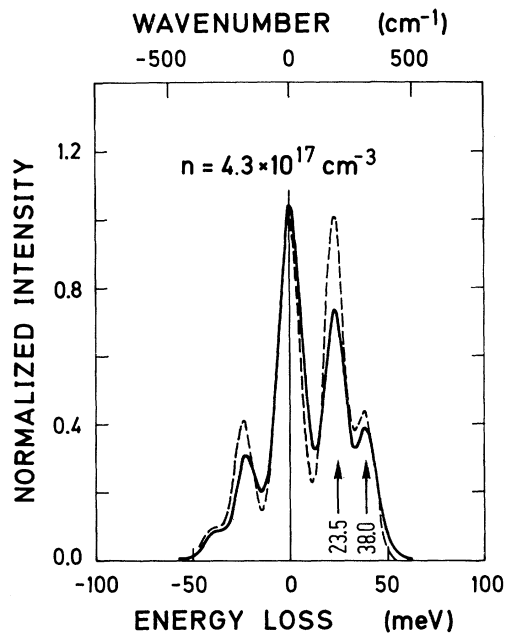


FIG. 3. Loss spectra calculated from Eq. (4) (Ref. 10), with use of Lindhard's dielectric function $\epsilon(\omega, q)$ superimposed on the TO lattice oscillator. Full line: Single-particle scattering included. Broken line: Single-particle scattering not included. Experimental peak positions (in meV) are given by arrows.

half angle of acceptance cone are shown with (curve in solid line) and without (curve in broken line) decay of the coupled eigenmodes $\hbar\omega_+$ and $\hbar\omega_-$ into electron-hole pairs. Plasmon dispersion and damping in the long-wavelength region due to finite electronic mobility have been neglected in Lindhard's $\epsilon(\omega, q)$; furthermore q transfer parallel to the surface (q_{\parallel}) only is considered. The peak positions $\hbar\omega_+$ and $\hbar\omega_-$ obtained for different carrier concentrations in this more quantitative model coincide with those from Drude's $\epsilon(\omega)$ (Fig. 2) within about 1%. The type of spectrum

in Fig. 1(b) is better described by taking intra-band scattering into account (Fig. 3, solid line). Nevertheless, care must be taken because of the assumptions involved. In particular, finite electronic mobility and plasmon dispersion might broaden the plasmonlike excitation and reduce its intensity further.

In conclusion, Fuchs-Kliwer surface phonon and conduction-band surface plasmons couple on infrared-active compound semiconductor surfaces. Further information about single-particle electron-hole-pair scattering might be obtained from HRELS measurements in off-specular direction. Another interesting point would be the quantitative correlation between band bending and frequency shift of the surface plasmon. Model calculations to this problem are already available.¹¹

The work was supported by the Deutsche Forschungsgemeinschaft (Sonderforschungsbereich 56).

¹R. Fuchs and K. L. Kliewer, Phys. Rev. **140**, 2076 (1965).

²H. Ibach, J. Vac. Sci. Technol. **9**, 713 (1972).

³R. Matz and H. Lüth, in *Proceedings of the European Conference on Surface Science, Cannes, 1980*, edited by D. A. Degras and M. Costa, Supplement No. 201 à la Revue "Le Vide, Les Couches Minces" (Société Française du Vide, Paris, 1980), p. 762.

⁴J. Geiger, *Elektronen und Festkörper* (Vieweg, Braunschweig, 1968).

⁵M. Hass and B. W. Henvis, J. Phys. Chem. Solids **23**, 1099 (1962).

⁶R. K. Willardson and A. C. Beer, *Semiconductors and Semimetals* (Academic, New York, 1967), Vol. III.

⁷M. Liehr and H. Lüth, J. Vac. Sci. Technol. **16**, 1200 (1979).

⁸E. Evans and D. L. Mills, Phys. Rev. B **5**, 4126 (1972).

⁹C. Kittel, *Quantum Theory of Solids* (Wiley, New York, 1963).

¹⁰D. L. Mills, Surf. Sci. **48**, 59 (1975).

¹¹S. L. Cunningham, A. A. Maradudin, and R. F. Wallis, Phys. Rev. B **10**, 3342 (1974).